

Stable half-metallic ferromagnetism in nonstoichiometric cubic binary chromium chalcogenides

San-Dong Guo and Bang-Gui Liu^(a)

Institute of Physics, Chinese Academy of Sciences, Beijing 100190, China
Beijing National Laboratory for Condensed Matter Physics, Beijing 100190, China

PACS 75.30.-m { Intrinsic properties of magnetically ordered materials
PACS 75.10.-b { General theory and models of magnetic ordering
PACS 75.90.+w { Other topics in magnetic properties and materials

Abstract.— We find that three nonstoichiometric cubic binary chromium chalcogenides, namely Cr_3S_4 , Cr_3Se_4 , and Cr_3Te_4 , are stable half-metallic ferromagnets with wide half-metallic gaps on the basis of systematic state-of-the-arts first-principles calculations. We optimize their structures, and then calculate their magnetic moments, electronic structures, formation heats, and elastic moduli and investigate their structural stability and robustness of ferromagnetism against antiferromagnetic fluctuations. Our calculated results show that the three sulvanite phases are structurally stable and ferromagnetically robust, and hence could be realized as epitaxial thin films. We attribute the structural and ferromagnetic stability and the better half-metallicity to their special effective Cr valence 2.667+. These findings will open doors for much more high-performance spintronic materials compatible with current semiconductor technology.

It is believed that next-generation high-performance computers can be achieved through using the spin freedom of electron in key materials and devices of current semiconductor technology [1, 2]. The half-metallic ferromagnet, first discovered in NiMnSb by de Groot et al in 1983, has almost 100% spin polarization near the Fermi level [3, 5]. This feature of half-metallic ferromagnetism makes carriers have high spin-polarization near the Fermi level and avoid some spin-related scattering processes that should exist otherwise. These are essential to practical spintronic applications [1, 2, 5]. Half-metallic ferromagnetism has been found in many materials, such as Heusler alloys [3, 4, 6], transition-metal oxides [7, 9], and even graphene nanoribbons under electric field [10]. The half-metallic ferromagnetic materials compatible with semiconductor technology is believed to be promising candidates for achieving more powerful computers. For this purpose, many zincblende transition-metal pnictides and chalcogenides [11–18], regularly-doped semiconductors [19, 20], semiconductor super-structures [21, 22], and more related compounds have been proved to be half-metallic. Although great advance has been achieved, better half-metallic ferromagnets compatible with cur-

rent semiconductor technology are highly desirable for the next-generation computers.

Here we find three stable half-metallic ferromagnets, namely Cr_3S_4 , Cr_3Se_4 , and Cr_3Te_4 , among nonstoichiometric cubic binary transition-metal chalcogenides on the basis of state-of-the-arts first-principles calculations. We investigate their structural stability and ferromagnetic robustness against antiferromagnetic fluctuations. Our calculated results show that the three nonstoichiometric sulvanite phases have formation heats of down to -0.302 eV per formula unit with respect to corresponding zincblende phases and their half-metallic gaps can be up to 1.05 eV. We attribute the structural and ferromagnetic stability and the better half-metallicity to their special effective Cr chemical valence 2.667+, compared with 2+ in the stoichiometric structures. These nonstoichiometric cubic materials have much better features for spintronic applications based on semiconductors. More detailed results will be presented in the following.

We use the full-potential linearized augmented-plane-wave method within the density functional theory (DFT) [23], as implemented in package WIEN2k [24, 25]. The generalized gradient approximation (GGA) [26] is used for the exchange-correlation potential. Full relativistic effects are calculated with the Dirac equations for core states,

^(a) E-mail: bgliu@mail.iphy.ac.cn

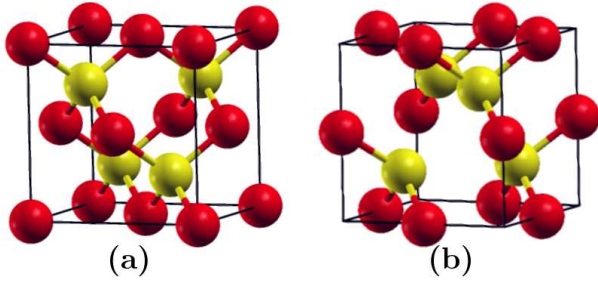


Fig. 1: (color online). The crystal structures of zincblende CrX (a) and sylvanite Cr_3X_4 (b) phases, where X can be S, Se, or Te. The red (or black) ball denotes a Cr atom and the yellow (or gray) an X atom.

and the scalar relativistic approximation is used for valence states. The spin-orbit coupling is neglected because it has little effect on our results. We use 2000 k points in the first Brillouin zone, make the harmonic expansion up to $l_{\text{max}}=10$ in atomic spheres, and set $R_{\text{mt}}/K_{\text{max}}$ to 7.5. The radii of the atomic spheres of Cr and others are chosen so that as high accuracy as possible is obtained. The volumes are optimized in terms of total energy, and the internal position parameters with a force standard of 3 mRy/a.u. The simplest antiferromagnetic structures are constructed by doubling the unit cells along the $[100]$ and $[110]$ directions. There are six Cr atoms in each of these doubled cells. We let three of the six Cr spins orient up and the other three down. All the spin values of the Cr, S, Se, and Te atoms are determined naturally by the self-consistent calculations. The structural stability is investigated through deforming the structures (with the volumes fixed) along the three directions. The elastic moduli are calculated with the standard method implemented in WIEN2k [24,25]. The formation heats of the cubic sylvanite structures are calculated with respect to the crystalline Cr phase and the corresponding zincblende structures. The self-consistent calculations are considered to be converged only when the absolute integrated charge-density difference per formula unit between the two successive loops is less than $0.0001 |e|$, where e is the electron charge.

The ground-state phases for three stoichiometric CrX ($X = \text{S}, \text{Se}, \text{and Te}$) compounds are of nickel-arsenide (na) structure, but the zincblende (zb) structures of the CrX have been shown to be higher only by 0.28–0.36 eV per formula unit than the corresponding na ones [15], and therefore have very good stability. This actually stimulated experimental synthesis of zb-CrTe epitaxial thin

films with a thickness up to 100 nm [16]. The sylvanite structure of Cr_3X_4 still has cubic symmetry with space group No. 215. Each of the cations has four anionic neighbors, but each of the anions three cationic neighbors. With the cations being at the $(\frac{1}{2}, 0, 0)$ sites, the anions occupy the (z_X, z_X, z_X) sites. The two cubic structures are shown in Fig. 1. For all the sylvanite Cr_3X_4 compounds, the

Table 1: The lattice constants a , the internal atomic parameters z_X , and the Cr-X bond lengths l_X of the three sylvanite Cr_3X_4 phases. Presented in parentheses are those of the corresponding zb-CrX phases.

Name	Cr_3S_4 (CrS)	Cr_3Se_4 (CrSe)	Cr_3Te_4 (CrTe)
a (Å)	5.344 (5.469)	5.679 (5.833)	6.117 (6.292)
z_X	0.250 (0.25)	0.250 (0.25)	0.260 (0.25)
l_X (Å)	2.315 (2.368)	2.460 (2.526)	2.686 (2.725)

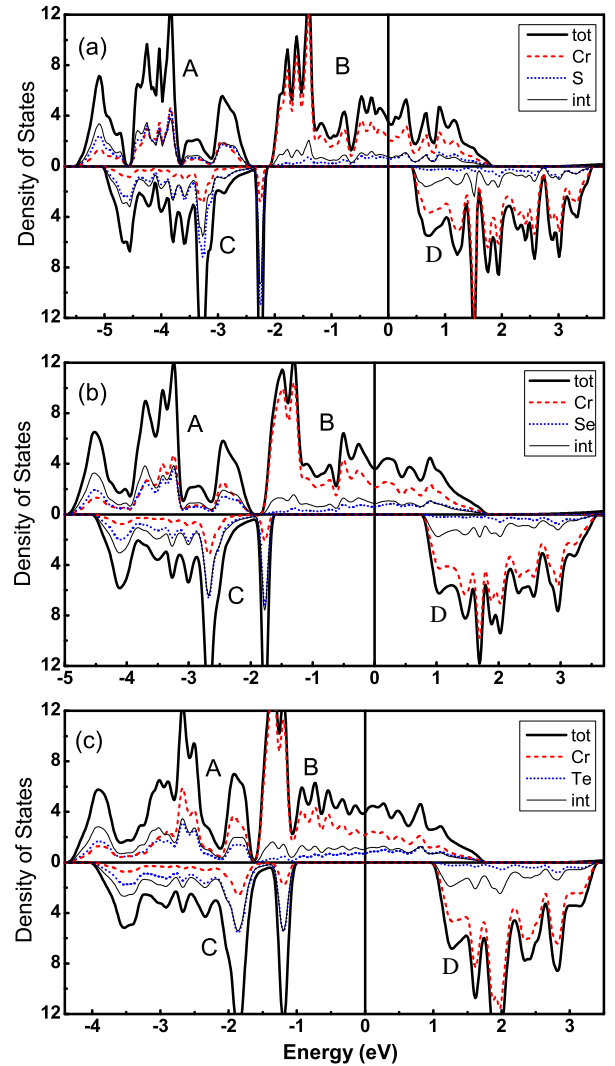


Fig. 2: (color online). Spin-dependent densities of states (DOSs) of the three sylvanite Cr_3X_4 phases for $X = \text{S}$ (a), Se (b), and Te (c). The upper part in each of the three panels is the majority-spin DOS and the lower part the minority spin. The solid thick line represents the total DOS; the red (or gray) dash, blue (or light gray) dot, and black thin lines describe the partial DOS projected in Cr and X atom spheres and the interstitial region, respectively.

lattice constant a and the internal structural parameter z_X are optimized fully in terms of usual total energy and force standards, and then the Cr-X bond lengths l_X are calculated with the optimized structures. We present our calculated a , z_X , and l_X results for all the three sylvanite Cr_3X_4 in Table 1. Those of the corresponding zb-CrX phases are shown in parentheses for comparison. Cr_3S_4 and Cr_3Se_4 almost keep the same $z_X = 0.25$ as zb-CrS and zb-CrSe, and Cr_3Te_4 has $z_X = 0.260$, a little larger than that of zb-CrTe. The sylvanite structures have smaller lattice constants than the zb ones by 1.6-2.6% and smaller Cr-X bond lengths by 1.4-2.6%. In the following, spin-dependent densities of states (DOSs), energy bands, and charge and moment density distributions are calculated in terms of the optimized structures.

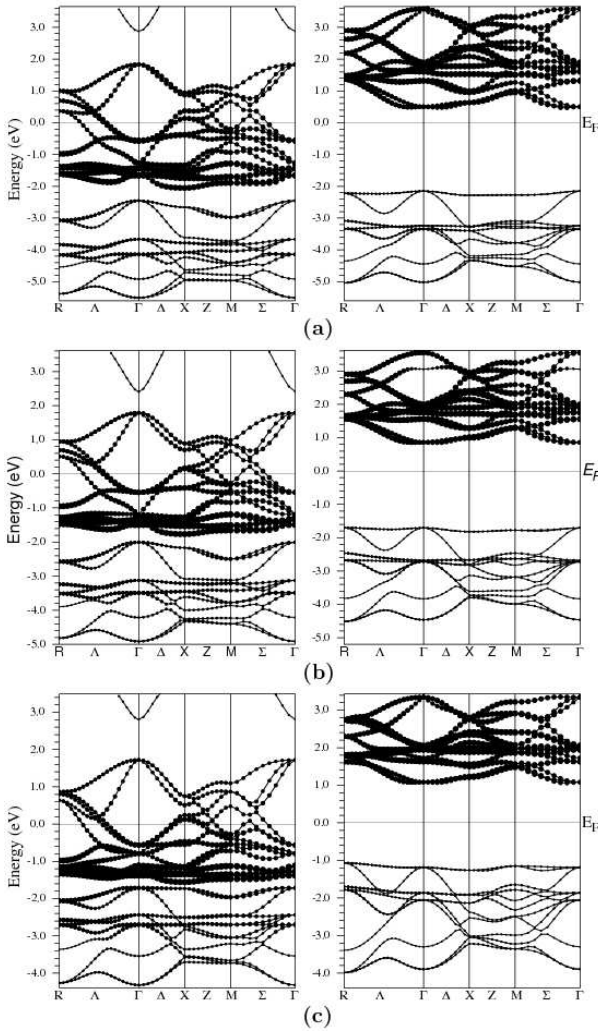


Fig. 3: Spin-dependent energy band structures (EBs) of the three sylvanite Cr_3X_4 phases for $X = \text{S}$ (a), Se (b), and Te (c). The left part in each of the three cases is the majority-spin bands and the right part the minority spin. The solid line with dots describes the EB structure along the high-symmetry points and the dot diameter is proportional to the Cr d weight at that point.

The spin-dependent DOSs of the three sylvanite Cr_3X_4 ($X = \text{S}, \text{Se}, \text{and Te}$) phases are presented in Fig. 2. For the convenience of description, we label the four different sets of the energy bands as A, B, C, and D, respectively. For each of the three X cases, there is a narrow gap between A and B in the majority-spin (MAS) channel and a wide gap between C and D in the minority-spin (MIS). It is clear that there is a gap across the Fermi level in the MIS channel for each of all the three cases and therefore all the three are half-metallic ferromagnets. In addition to the total DOS, partial DOSs projected in the muffin-tin spheres of Cr and X atoms and in the interstitial region are presented too. It is clear that the B and D bands are originated from Cr-d states and the A and C bands mainly have the X-p (S, Se, or Te) character.

Presented in Fig. 3 are the spin-dependent energy bands, according to the corresponding DOS plots in Fig. 2, for $X = \text{S}, \text{Se}, \text{and Te}$. There are twelve bands in both A and C. They result from the fact that we have four X (S, Se, or Te) atoms in the sylvanite Cr_3X_4 unit cell and each of the four has three p orbitals. There are fifteen bands in both B and D because we have three Cr atoms here and each of the three has five d orbitals. The e_g bands are lower than the t_{2g} ones. The Cr-s state is put to higher energy than the B and D bands in both of the MAS and MIS channels. This is in contrast with zb-CrX phases whose Cr-s states are merged with the Cr-d t_{2g} states. We have also calculated charge and spin densities in three typical planes. Our results show that the charge density from the A and C bands is distributed mainly in the neighborhoods of the X and Cr atoms, but the spin density is almost limited to Cr and X atoms only. The filled part of the B bands are substantially localized near Cr and X atoms. When X changes from S to Te, the X-p character becomes less and less in the electron density from the filled B bands because the ionic radius becomes larger and larger.

Table 2: The magnetic moments (M), half-metallic gaps (G_{HM}), magnetic energy differences (E), formation heats (H_{Fom}), and the elastic moduli (B , C^0 , and C_{44}) of the three Cr_3X_4 phases, compared with the zb-CrX phases (in parentheses).

Name	Cr_3S_4 (CrS)	Cr_3Se_4 (CrSe)	Cr_3Te_4 (CrTe)
M (μ_B)	10 (4)	10 (4)	10 (4)
G_{HM} (eV)	0.50 (0.07)	0.83 (0.61)	1.05 (1.00)
E (eV)	0.57	0.56	0.11
H_{Fom} (eV)	-0.148	-0.114	-0.302
B (GPa)	72.9 (63.2)	57.7 (59.5)	44.1 (45.9)
C^0 (GPa)	8.8	5.9 (5.6)	4.8 (5.5)
C_{44} (GPa)	34.2	35.9 (50.7)	32.9 (36.4)

We summarize in Table 2 the total moments per formula unit (M), half-metallic gaps (G_{HM}) [27], and the energy differences per formula unit ($E = E_{\text{AF}} - E_{\text{FM}}$)

- [1] S. A. Wolf, D. D. Awschalom, R. A. Buhrman, J. M. Daughton, S. von Molnar, M. L. Roukes, A. Y. Chtchelkanova, and D. M. Treger, *Science* 294 (2001) 1488.
- [2] W. E. Pickett and J. S. Moodera, *Phys. Today* 54 (2001) 39.
- [3] R. A. de Groot, F. M. Mueller, P. G. van Engen, and K. H. J. Buschow, *Phys. Rev. Lett.* 50 (1983) 2024.
- [4] J. J. Aumentado, G. A. de Wijs, and R. A. de Groot, *J. Phys.: Condens. Matter* 19 (2007) 315212.
- [5] W. E. Pickett and H. Eschrig, *J. Phys.: Condens. Matter* 19 (2007) 315203.
- [6] E. Kisker, C. Carbone, C. F. Flipse, and E. F. Wassenmann, *J. Magn. Magn. Mater.* 70 (1987) 21; J. S. Correa, Ch. Eibl, G. Rangelov, J. Braun, and M. Donath, *Phys. Rev. B* 73 (2006) 125316.
- [7] K.-I. Kobayashi, T. Kimura, H. Sawada, K. Terakura, and Y. Tokura, *Nature (London)* 395 (1998) 677.
- [8] S. M. Watts, S. Wirth, S. von Molnar, A. Barry, and J. M. D. Coey, *Phys. Rev. B* 61 (2000) 9621; S. Soeya, J. Hayakawa, H. Takahashi, K. Ito, C. Yamamoto, A. Kida, H. Amano, and M. Matsui, *Appl. Phys. Lett.* 80 (2002) 823.
- [9] J. M. D. Coey, M. Viret, and S. von Molnar, *Adv. Phys.* 48 (1999) 167.
- [10] Y. W. Son, M. L. Cohen, and S. G. Louie, *Nature* 444 (2006) 347.
- [11] S. Sanvito and N. A. Hill, *Phys. Rev. B* 62 (2000) 15553.
- [12] H. Akinaga, T. Manago and M. Shirai, *Jpn. J. Appl. Phys.*, part 2, 39 (2000) L1118; M. Mizuguchi, H. Akinaga, T. Manago, K. Ono, M. Oshima, M. Shirai, M. Yuri, H. J. Lin, H. H. Hsieh, and C. T. Chen, *J. Appl. Phys.* 91 (2002) 7917.
- [13] J. H. Zhao, F. Matsukura, K. Takamura, E. Abe, D. Chiba, and H. Ohno, *Appl. Phys. Lett.* 79 (2001) 2776.
- [14] Y.-Q. Xu, B.-G. Liu, and D. G. Pettifor, *Phys. Rev. B* 66 (2002) 184435; B.-G. Liu, *Phys. Rev. B* 67 (2003) 172411.

- [15] W.-H. Xie, Y.-Q. Xu, B.-G. Liu, D. G. Pettifor, *Phys. Rev. Lett.* 91 (2003) 037204.
- [16] M. G. Sreenivasan, K. L. Teo, M. B. A. Jalil, T. Liew, T. C. Chong, and A. Y. Du, *IEEE Trans. Magn.* 42 (2006) 2691; M. G. Sreenivasan, J. F. Bi, K. L. Teo, and T. Liew, *J. Appl. Phys.* 103 (2008) 043908; J. F. Bi, M. G. Sreenivasan, K. L. Teo, and T. Liew, *J. Phys. D: Appl. Phys.* 41 (2008) 045002.
- [17] J. F. Bi, J. H. Zhao, J. J. Deng, Y. H. Zheng, S. S. Li, X. G. Wu, and Q. J. Jia, *Appl. Phys. Lett.* 88 (2006) 142509.
- [18] J. J. Deng, J. H. Zhao, J. F. Bi, Z. C. Niu, F. H. Yang, X. G. Wu, and H. Z. Zheng, *J. Appl. Phys.* 99 (2006) 093902; S. D. Li, J.-G. Duh, F. Bao, K.-X. Liu, C.-L. Kuo, X. S. Wu, L. Y. Lu, Z. G. Huang, and Y. W. Du, *J. Phys. D: Appl. Phys.* 41 (2008) 175004; S. D. Li, Z. J. Tian, J. L. Fang, J.-G. Duh, K.-X. Liu, Z. G. Huang, Y. H. Huang, Y. W. Du, *Solid Stat. Commun.* 149 (2009) 196.
- [19] H. Ohno, *Science* 281 (1998) 951; T. Dietl, H. Ohno, F. Matsukura, J. Cibert, and D. Ferrand, *Science* 287 (2000) 1019.
- [20] L.-J. Shi and B.-G. Liu, *Phys. Rev. B* 76 (2007) 115201; L.-F. Zhu and B.-G. Liu, *J. Phys. D: Appl. Phys.* 41 (2008) 215005; L.-J. Shi, L.-F. Zhu, Y.-H. Zhao, and B.-G. Liu, *Phys. Rev. B* 78 (2008) 195206.
- [21] M. C. Qian, C. Y. Fong, K. Liu, W. E. Pickett, J. E. Pask, and L. H. Yang, *Phys. Rev. Lett.* 96 (2006) 027211.
- [22] P. Mavropoulos, M. Lezaic, and S. Blügel, *Phys. Rev. B* 72 (2005) 174428.
- [23] P. Hohenberg and W. Kohn, *Phys. Rev.* 136 (1964) B864; W. Kohn and L. J. Sham, *Phys. Rev.* 140 (1965) A1133.
- [24] P. Blaha, K. Schwarz, P. Sorantin, and S. B. Trickey, *Comput. Phys. Commun.* 59 (1990) 399.
- [25] P. Blaha, K. Schwarz, G. K. H. Madsen, D. Kvasnicka, and J. Luitz, *WIEN2k* (K. Schwarz, Tech. Univ. Wien, Austria) (2001), ISBN 3-9501031-1-2.
- [26] J. P. Perdew, K. Burke, and M. Ernzerhof, *Phys. Rev. Lett.* 77 (1996) 3865.
- [27] B.-G. Liu, *Half-Metallic Ferromagnetism and Stability of Transition Metal Pnictides and Chalcogenides*, in: I. Galanakis and P. H. Dederichs (Eds.), *Half-metallic alloys – Fundamentals and applications* (Springer Berlin 2005), *Lecture Notes in Physics* 676 (2005) 267-291.